Review Article

Ning Li[#], Li Zhang[#], Ou Qiao, Xinyue Wang, Linyan Xu, and Yanhua Gong*

Special contribution of atomic force microscopy in cell death research

https://doi.org/10.1515/ntrev-2023-0208
received August 24, 2023; accepted January 25, 2024

Abstract: Cell death is an important life activity in individual development. Changes in morphological and mechanical properties during cell death are crucial to identify the modes of cell death. However, due to technical limitations, little is known about these characteristics. The emergence of atomic force microscopy (AFM), a nanoscale research tool that integrates imaging and mechanical measurement functions, provides new insights into our understanding of cell death. Based on a brief introduction to the structure, principle, and working modes of AFM, this article elaborates on the contribution of AFM in cell death to detect morphological and mechanical properties, especially in apoptotic cells. Meanwhile, the potential of AFM in distinguishing different cell death modes and visualizing membrane pores (medicated by apoptosis and pyroptosis) is illustrated. In addition, this article states that using single-molecule force spectroscopy by AFM to study the mechanical and adhesive properties of cell death-related molecules. Finally, we discuss the challenges facing and further perspective of AFM.

Keywords: atomic force microscopy, cell death, cell morphology, cell mechanical properties, membrane pores, single-molecule force spectroscopy by AFM (AFM-SMFS)

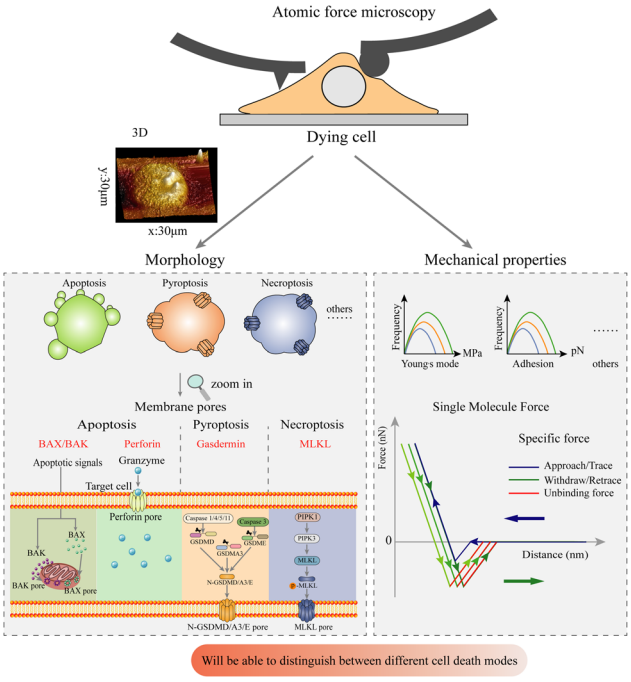

Graphical abstract

Abbreviations

AFM	atomic force microscopy
AFM-SMFS	single-molecule force spectroscopy by AFM
PCD	programmed cell death
MP-AFM	multiparametric imaging AFM
HS-AFM	high-speed AFM
STM	scanning tunneling microscope
OM	optical microscopy
TEM	transmission electron microscopy
SEM	scanning electron microscopy
STS	staurosporine
IV	chrysin-organogermanium
Chry-Ge	chrysin-organogermanium complex
SNP	sodium nitroprusside
MOM	mitochondrial outer membrane
PFR	perforin
MAC	membrane attack complex
MOMP	mitochondrial outer membrane permeability
SLBs	supported lipid bilayers
SLMs	supported lipid membranes
MR-AFM	molecular recognition AFM
MF-AFM	multifrequency AFM

# These authors contributed equally to this work and should be considered first co-authors.

* **Corresponding author: Yanhua Gong,** Institute of Disaster and Emergency Medicine, Medical School, Tianjin University, Tianjin, 300072, China, e-mail: gongyanhua@tju.edu.cn, tel: +8622 27893596
Ning Li, Li Zhang, Ou Qiao, Xinyue Wang: Institute of Disaster and Emergency Medicine, Medical School, Tianjin University, Tianjin, 300072, China
Linyan Xu: State Key Laboratory of Precision Measuring Technology and Instruments, Medical School, Tianjin University, Tianjin, 300072, China

FluidFM	fluidic force microscopy
QI™	Quantitative Imaging™
SMLM	single-molecule localization microscopy

1 Introduction

Cell death is a ubiquitous biological phenomenon in all living organisms and is inseparable from organ development, aging, and the removal of damaged cells [1,2]. Research on the process of cell death has become a research hotspot in the fields of biology, medicine, and pharmacy. Based on functional differences, cell death can be classified into two types: programmed cell death (PCD) and non-PCD (necrosis) [3]. Currently known PCDs mainly include apoptosis, necroptosis, pyroptosis, autophagy, ferroptosis, and so on. The molecular mechanisms/signaling pathways of different death modes have been extensively explored, and meanwhile, morphological and mechanical properties are also particularly important for the characterization of different death modes. Especially in the field of oncology research, alterations in the elasticity and adhesion of individual cancer cells have been recognized as a property that promotes the spread of cancer cells [2,4–6]. The morphological characteristics and mechanical properties of classical cell death modes such as apoptosis have been initially explored, but the morphological and mechanical properties of new cell death modes have not been fully analyzed.

Atomic force microscopy (AFM) is a nanoscale research tool that integrates imaging and mechanical measurement functions [7]. Compared with other traditional microscopy techniques, AFM has many advantages. For example, in terms of sample imaging, the imaging environments are diverse, and samples can be imaged under various conditions, such as air, vacuum, or liquid, including dynamic observation of living cells [8,9]. In addition, the sample is not limited by its conductive properties. Moreover, AFM does not require staining, labeling, or fixing. The possibility to operate in liquid environments and at ambient temperature moved the application of AFM extends from the materials science to the biological science [10], which needs to overcome many difficulties, including the difference between material samples and biological samples. In general, the preparation of biological samples is more complex, such as the preparation of suspension cell samples, which needs to use diverse methods (such as electrostatic adsorption and microporous membrane filtration) to fix the cells to the substrate (such as Petri dishes, cover slides) [11]. During imaging of certain biological samples, such as membrane proteins protruding ~1 nm from the membrane, the AFM contact mode can provide sub-nanometer resolution (≤1 nm) for imaging individual membrane proteins [8–10,12,13]. Meanwhile, various physical, chemical, and biological parameters can be characterized during imaging. In addition, as a multifunctional tool, AFM is one of the important tools to study the mechanical properties of cells, including the measurements of cell Young's modulus, adhesion, and viscoelasticity [14–16]. And AFM can measure the rupture forces between molecules or particles in the piconewton (pN) range, such as analyzing the interaction force of receptor–ligand [17–20]. Over the past few decades, AFM has been successfully applied to the imaging analysis of various biological systems, including nucleic acids [21], proteins [22], cells [23,24], and tissues [23,25].

At the same time, recent research advances in AFM technology have strengthened its capabilities, such as multiparametric imaging AFM (MP-AFM) [26], and high-speed AFM (HS-AFM) [27], which enables simultaneous multiparametric imaging in a short time. The extraordinary ability of AFM makes it show a very broad contribution prospect in the field of cell death. It can clearly observe the morphological changes of different cell death methods, including changes in cell size, cell height, cell surface roughness, and the formation of cell membrane pores. In addition, AFM can measure dynamic changes in mechanical properties during cell death. Based on the previous research, this article briefly introduces the basic structure, imaging principle, and working modes of AFM and reviews its contribution in the field of cell death in detail, including the study of morphological and mechanical properties of different cell death modes (Graphical abstract, the curve in the figure is a schematic and does not represent real experimental data). At the end of this article, we also expound on the research status of AFM and discuss its current challenges and future development directions for the shortcomings of AFM.

2 The morphology and mechanisms of different cell death modes

There are multiple cell death modes, such as apoptosis, pyroptosis, necroptosis, and ferroptosis. Apoptosis was first described by Kerr *et al.* from a morphological point of view to describe the physiological death of cells and named it apoptosis [28]. The main morphological features of apoptotic cells are chromatin condensation, cell shrinkage, cell membrane blebbing, cell budding to form apoptotic bodies, *etc.* [2,28,29] (Table 1). After induction of apoptosis, BAX and BAK are activated and aggregated and inserted on the mitochondrial outer membrane (MOM), undergo conformational

Table 1: The morphological features of different cell death modes

Cell death modes	Apoptosis	Pyroptosis	Necroptosis	Ferroptosis
Morphological features	Cell shrinkage increased; numerous smaller apoptotic bodies [30]	Very swollen morphology and burst; pores form in the cell membrane [31]	Cells do not shrink but detach and swell; pores form in the cell membrane [30]	Circular protrusions formed on the membrane, about 1–5 μm [30,32]

rearrangement, oligomerize to form pores, and release pro-apoptotic factors such as cytochrome *C* and SMAC/DIABLO, *etc.*, thereby initiating the apoptotic program [33–36]. Then in 2001, Cookson *et al.* first proposed the definition of pyroptosis, which is described as pro-inflammatory PCD [37]. The main morphological manifestations were DNA breakage, cell swelling, cell membrane pore formation, and release of cell contents (Table 1). During pyroptosis, gasdermin D (GSDMD) or GSDME is activated by caspase-1/4/5/11 or caspase-3 after cleavage, oligomerization and inserts into the cell membrane to form pyroptotic pores, leading to cell swelling and rupture [38–40]. Afterward, in 2005, the necroptosis term was first proposed by Degterev *et al.* [41]. Its main features include cell membrane rupture, autophagosome formation, and significant organelle swelling. RIPK1, RIPK3, and MLKL are key molecules in the process of necroptosis. Researchers found that p-MLKL has the potential to create pores in the plasma membrane resulting in membrane rupture [42,43]. Ferroptosis as a novel cell death mode was first proposed in 2012 by Dixon *et al.* [44]. The morphological characteristics were cell membrane rupture, increased density, and decreased volume of the mitochondrial membrane [45] (Table 1).

3 Introduction to AFM structure, principle, and working modes

3.1 AFM structure and principle

AFM was invented by physicist Binnig *et al.* in 1986 [7]. The invention of AFM overcomes the shortcomings of STM in measuring nonconducting samples and expands the detection from conductors and semiconductors to insulators [7]. In addition, AFM has a wide range of applications compared to other microscopes, including working in liquid environments (PBS) as well as soft samples (living cells), combining topographic imaging with force spectroscopy and nanomechanics (Table 2). AFM mainly consists of the following systems: a laser system for laser generation, a head detection system consisting of a cantilever and a very sharp tip at its end, a laser detection system that receives laser reflection, and a feedback system that processes and transmits feedback signals to the piezoelectric scanner. The working principle of AFM is shown in Figure 1a. When the tip of the probe begin to scan the sample, the weak interaction force (mechanical contact force, van der Waals force, electrostatic force, *etc.*) between the probe tip and the sample causes the cantilever to swing. The deformation signal is converted into a photoelectric signal and amplified, and the signal of the interaction force between

Table 2: Comparison of AFM and other high-resolution techniques

Characteristics	AFM [10,46,47]	Super-resolution microscopy (SLML) [48–51]	Transmission electron microscopy [46,52]	Scanning electron microscopy [10,46]
Resolution	≤1 nm	<10 nm	0.2 nm	1 nm
Sample preparation	Sample on supported.	Organic dyes or fluorescence labeling.	Sample onto a grid.	Freezing or critical point drying and metal spraying.
Advantages	Imaging conditions are native; high signal-to-noise ratio; without staining, labeling, or fixing.	Monitoring of dynamic cellular or biomolecular movements; high spatial and temporal resolution; visualization of subcellular structures.	Imaging individual nanoscale objects in real space and reciprocal space.	Imaging features of the sample surfaces.
Limitation	Limited to surfaces.	Imaging produces photobleaching and phototoxicity.	Imaging in a vacuum environment; the specimen must be thin.	Imaging in a vacuum environment.

atoms can be obtained. Among them, the interaction force between the tip and the sample is related to the distance between them, which can be simply divided into attractive force and repulsive force, as shown in Figure 1b.

3.2 AFM working modes

AFM provides three commonly used working modes, namely contact mode, non-contact mode, and dynamic mode (originally called tapping or oscillation mode), as shown in Figure 1c. In the contact mode, the sample and the tip are always in contact (corresponding to segments 1–2 in Figure 1b). In this mode, high-resolution images can be obtained due to the close proximity of the sample to the tip [53]. But also because of this, too close distance may cause contamination and damage to the tip, and the friction force of the tip to the sample will also cause damage to the sample and affect the quality of imaging [54]. Therefore, when applying it to softer biological samples, it is necessary to adjust the force applied to the tip, generally avoiding more than 100 pN, as excessive force may lead to reversible or even irreversible deformation [55–57]. In the non-contact mode, the microcantilever vibrates near the sample surface (corresponding to segments 3–4 in Figure 1b) [58]. In this mode, the tip is not in direct contact with the sample, which makes up for the problems of sample damage and tip contamination in the contact mode. However, compared with the contact mode, the non-contact mode has a lower resolution and is unsuitable for imaging in liquid environments. In the dynamic mode, the cantilever oscillates with a larger amplitude (greater than 20 nm) near the resonance frequency during the scanning process (corresponding to segments 1–4 in Figure 1b). This mode minimizes friction and shear forces between the tip and the sample while maintaining a resolution that is essentially the same as the contact mode. In summary, the dynamic mode is suitable for objects that are more flexible and more brittle and only weakly adsorb to supports, such as DNA [59,60], proteins [61], and fibrils of Tau [62].

4 Use AFM to detect the dynamic changes of morphological and mechanical properties of different cell death modes

Some caution should be taken into account to reduce the invasiveness degree toward the delicate biological cell

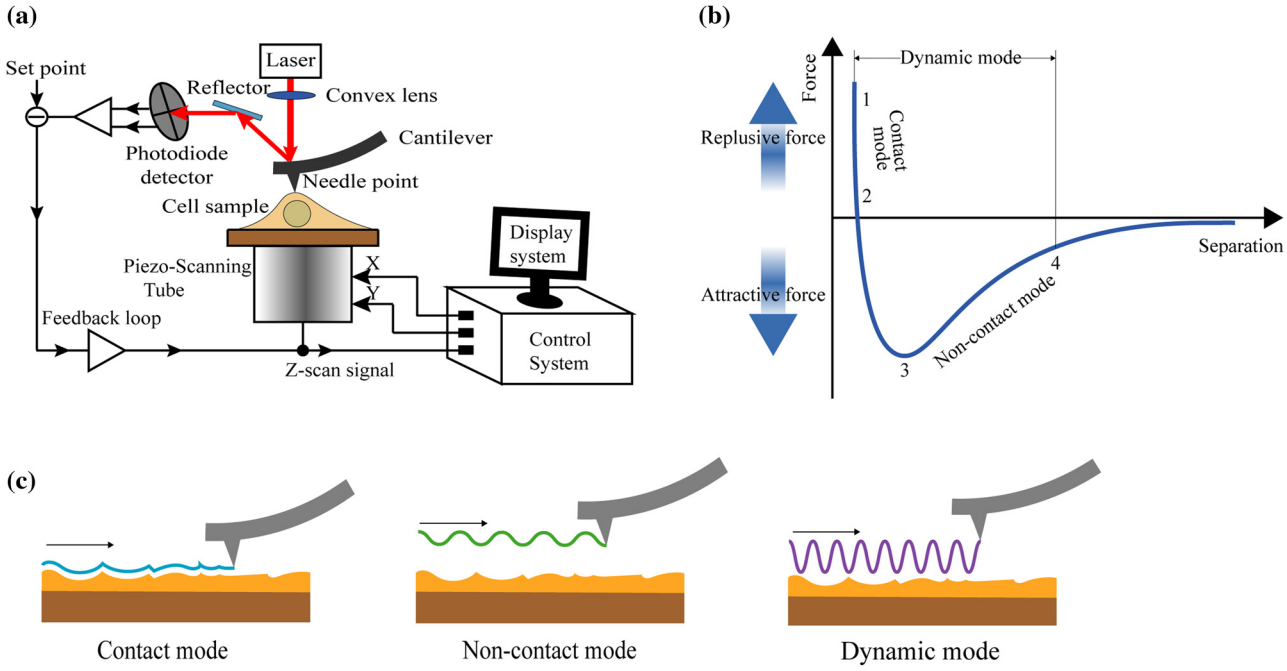

Figure 1: AFM. (a) Schematic diagram of AFM operation. (b) Force–distance curve by AFM. (c) Three working modes are commonly used in AFM.

samples during AFM technique. The first is sample preparation. In living cells, the position change of the sample caused by the lateral force applied by the AFM probe during scanning imaging should be avoided [63]. For adherent cells, because they can be naturally attached to the substrate (such as Petri dishes, cover slides), they can be directly imaged after adherent [64]. The substrate surface can also be covered with a layer of polylysine to increase the adhesion effect [65]. For suspension cells, appropriate fixation methods (such as electrostatic adsorption and microporous membrane filtration) are needed to adsorb them to the substrate and then image them [11]. The second is the choice of probe. Probe quality and probe parameters will directly affect the final result. Because of its small contact area with the cell, the pyramidal probe can capture the details of the geometric properties of the cell surface and is often used for cell surface topography scanning [66]. The micrometer-sized spherical probe is often used to measure the more holistic mechanical properties of cells because of their stable contact [66].

4.1 AFM exploring the morphological characteristics of apoptotic cells

Human understanding of cell death has gone through a long process. Prior to the advent of cell staining and microscopy, early studies of cell death largely focused on morphological observations with the naked eye [67,68]. So far, morphological observation is still one of the important basis for judging different cell death modes. And different death modes show different morphological characteristics. Currently, cell morphology is mainly observed by optical microscopy (OM), transmission electron microscopy (TEM), and scanning electron microscopy (SEM), but these methods all have certain limitations [69–71] (Table 2). For example, conventional OM suffers from a resolution limit of 200 nm, making it impossible to reveal the nanostructure of cells [72,73]. Second, the essential advantage of AFM over TEM/SEM is the ability to measure the biophysical properties of biological samples under physiological conditions [74]. In recent years, with the development of microscopy technology, AFM has been gradually applied to the morphological observation of different cell death modes. According to the obtained 2D and 3D topological maps of cells, relevant information such as cell volume, cell height, cell membrane surface roughness, and cell membrane pore formation can be clearly collected, which provides a strong support for further understanding the morphological characteristics of specific cell death modes.

AFM has been used to observe the morphological characteristics of different cell death modes, but existing studies have mainly focused on apoptosis. Previous studies have shown that reduction in cell volume is a prerequisite for the early stages of apoptosis [75–77]. In 2005, Hessler

et al. used AFM to observe early morphological changes in human oral epidermoid carcinoma cells (KB cells) apoptosis induced by staurosporine (STS) [77]. The images were obtained using the contact mode by silicon nitride cantilevers MSCT-AUNM (cantilever C) at the spring constant of about 0.01 N m^{-1}. AFM data showed a 50% reduction in total cell volume and a 32% reduction in total cell height, and the reduction in apoptotic cell volume preceded other key hallmarks of apoptosis, such as loss of mitochondrial membrane potential [77]. Researches also indicated that there was a significant change in cell volume during the initial stage of apoptosis [77]. Cells are generally in the range of an AFM scan, but even the same cell type can vary by up to a few micrometers. Therefore, there are many difficulties that need to be overcome in using changes in cell volume as a marker of early apoptosis. However, it is much more convenient to observe the surface characteristics of the membrane. Moreover, the variation of cell membrane surface roughness is an indication of early apoptosis. AFM morphological imaging allows the extraction of 3D topology-related data of cells, which enables analysis of cell membrane surface roughness. Therefore, to identify apoptosis at an early stage, in 2011, Wang *et al.* employed AFM to observe changes in the membrane surface roughness of hydrogen peroxide (H_2O_2)-induced apoptosis in the mouse macrophage cell line RAW264.7 [78]. Results showed that the mean roughness increased between 24 and 60 nm with increasing H_2O_2 concentration [78]. It is worth noting that, although under normal circumstances, with the occurrence of apoptosis, the surface roughness of the cell membrane shows an increasing trend. However, there are some exceptions. For example, when Cai *et al.* used AFM to observe the apoptotic K562 cells induced by peripheral lymphocytes. The UL20B cantilever whose length, width, and thickness are 115, 30, and 3.5 μm, respectively, was chosen in the contact mode. The oscillation frequency is 255 kHz and the force constant is 0.01 N m^{-1}. And they found that after co-culturing these two type cells, K562 cells showed typical characteristics of apoptosis, but the cell surface roughness was significantly reduced [79]. Furthermore, the formation of cell membrane pores is one of the sources of cell surface roughness, and as the pores become deeper, the cell surface becomes rougher [80]. Therefore, to better describe the morphological characteristics of apoptosis, cell membrane pores are usually observed and analyzed. These studies further reveal morphological changes during apoptosis and deepen our understanding of cell death.

4.2 Advances in AFM measurement of mechanical properties during cell death

Likewise, cell mechanics can be used to describe the state of a cell, where certain changes in mechanical properties occur during cell death. AFM has been shown to be a powerful non-destructive nanotechnology that can be used to obtain dynamic processes related to cellular mechanics, such as elasticity and adhesion. Studies have shown that apoptosis may be associated with changes in cell elasticity [81]. In addition, the adhesion of cell membranes plays a very important role in cell physiology and pathological processes. Hu *et al.* used AFM measurement and calculated by Hertz model to obtain the Young's moduli of lymphocytes in three states of resting, activated, and apoptotic, which were 11.2 ± 5.9, 19.7 ± 4.0, and 7.1 ± 4.1 kPa, respectively, indicating that the Young's modulus of apoptotic cells was significantly reduced [82]. The high values of the Young's modulus of elasticity reported in this article may be due to the limitations of experimental conditions, such as force profiles measured in air, where humidity, temperature, cell dehydration, or cell drying can have a dramatic effect on the results. For example, in 2014, Jin *et al.* showed the damaged effect of sodium nitroprusside (SNP) on cell surface adhesion (30% reduction) and elasticity (90% reduction) at the nano level in apoptotic chondrocytes [83]. In this study, the force spectrum experiment was performed at the force loading rate is 1.2×10^5 pN s^{-1}. The mechanical properties of cells have gradually become an important characteristic to distinguish healthy cells from dead cells. Meanwhile, due to the extremely high mechanical resolution of AFM, AFM single-molecule force spectroscopy technology (AFM-SMFS) developed in AFM technology has gradually become an effective tool to measure the intra- and inter-cellular interactions of biological macromolecules at the single-cell level. Future AFM holds great potential for the mechanistic measurement of different cell death modes.

4.3 Use AFM to study the relationship between cell death and cytoskeleton

In the process of studying cell mechanics, the study of the cytoskeleton is an essential part. The cytoskeleton is important for maintaining cell mechanical properties [84], and cytoskeleton remodeling plays an important role in the process of apoptosis [30,85]. Importantly, it has been shown that

changes in cellular elasticity are inextricably linked to the components of the cytoskeleton in addition to the intrinsic properties of the cell membrane [86]. Actin filaments and microtubules, two major components of the cytoskeleton, are severely damaged in structure, organization, and function, leading to cell death [74]. For example, Jin *et al.* studied the cytoskeleton of SNP-induced chondrocyte apoptosis, and after SNP treatment, the F-actin and α-tubulin cytoskeleton of chondrocytes reorganized and polymerized [83]. In addition, other researchers have continued to explore how the composition of the cytoskeleton affects cell elasticity. Rotsch and Radmacher found drugs that depolymerized actin filaments could significantly reduce the elastic modulus of cells, while drugs that stabilized microtubules had no significant effect on cell elasticity, suggesting that the actin network primarily determines the elastic properties of living cells [87]. To learn more about the effects of how microtubules and actin filaments affect cytoskeletal mechanical properties during apoptosis. Pelling *et al.* indicated that cell structure was highly dynamic during the early stages of apoptosis, with F-actin in actin filaments controlling the cell's initial elastic response, while microtubules appear to control the cell's viscous relaxation for extended periods [88]. Due to the limitations of AFM imaging, the most common way to monitor cytoskeletal changes is to combine AFM with confocal microscopy to study the dynamic changes of actin filaments and microtubules. However, the study by Henderson *et al.* showed that AFM could directly image actin filaments in living cells and observe the dynamic changes of actin filaments [89]. Although researchers have a preliminary understanding of the role of the cytoskeleton in maintaining the mechanical properties of cells, the relationship between the cytoskeleton and cell death remains to be further explored.

4.4 Potential of AFM to distinguish different cell death modes

With the development of AFM technology year by year, studies using AFM to observe various cell death modes have emerged in recent years [79,90,91]. Meeren *et al.* tested the differences in morphological and mechanical properties between three different PCD modes: intrinsic and extrinsic apoptosis, necroptosis, and ferroptosis in mouse tumor cell lines (L929sAhFas cell line) [30]. In morphological measurements, the resulting topographic image was obtained using the ATEC-CONT cantilever in a JPK QI® mode using the selected AFM nanowizard 4™ (JPK GmbH Instruments/Bruker). In cell elasticity measurements, all force curves were obtained in a contact mode using a colloidal probe containing a spherical tip of 5 μm diameter (CP-qp-SCONT-BSG, force constant 0.1 N m^{-1}) and using a setpoint of 2 nN at 2 μm s^{-1}. During intrinsic apoptosis, cells shrink and irregular structures are formed (Figure 2a, middle left). During extrinsic apoptosis, cell shrinkage was increased with concomitant apoptotic body generation (Figure 3a, middle right). During necroptosis, cells did not shrink but detached and swelled, and pores of different sizes were formed in the cell membrane (Figure 2b, middle). During ferroptosis, circular protrusions of 1–5 μm were observed to form on the cell membrane surface (Figure 2c, middle). In addition, the data showed that as the cell death process progressed, the cell surface roughness of these three cell death modes increased significantly. And the smallest increase is necroptosis. Overall, the AFM data clearly showed morphological characteristics in different cell death modes. Second, Meeren *et al.* also used AFM to measure the elasticity of multiple cells in these three PCDs. In the process of intrinsic apoptosis, Young's modulus decreased rapidly 15 min after induction (Figure 2a, bottom left) and remained basically stable after the decrease. In contrast, for extrinsic apoptosis, Young's modulus showed a trend of first increasing and then rapidly decreasing 60 min after induction (Figure 2a, bottom right). For both necroptosis and ferroptosis, Young's modulus showed a continuous decreasing trend (Figure 2b and c, bottom). When comparing the Young's modulus of these three cell death modes, it was found that the Young's modulus of apoptosis (intrinsic and extrinsic apoptosis) decreased more rapidly compared with necroptosis and ferroptosis. Therefore, using AFM to study different cell death modes will help us to more clearly understand the dynamic changes of morphological and mechanical properties in the process of cell death.

5 AFM visualizes membrane pores in different cell death

A membrane pore can be defined as any local membrane perturbation that allows passive flow of molecules [96]. Different types of pores formation in the membrane may lead to different types of cell death [31]. For example, after induction of apoptosis, BAX and BAK will aggregate into pores in the mitochondrial membrane, release pro-apoptotic factors, and start the apoptosis process [34]. In addition, during apoptosis, perforin (PFR) released by T/NK cells can also form pores in the cell membrane [97]. Similarly, the gasdermin family (such as GSDMD or GSDME), the ultimate executor of pyroptosis, induces the occurrence

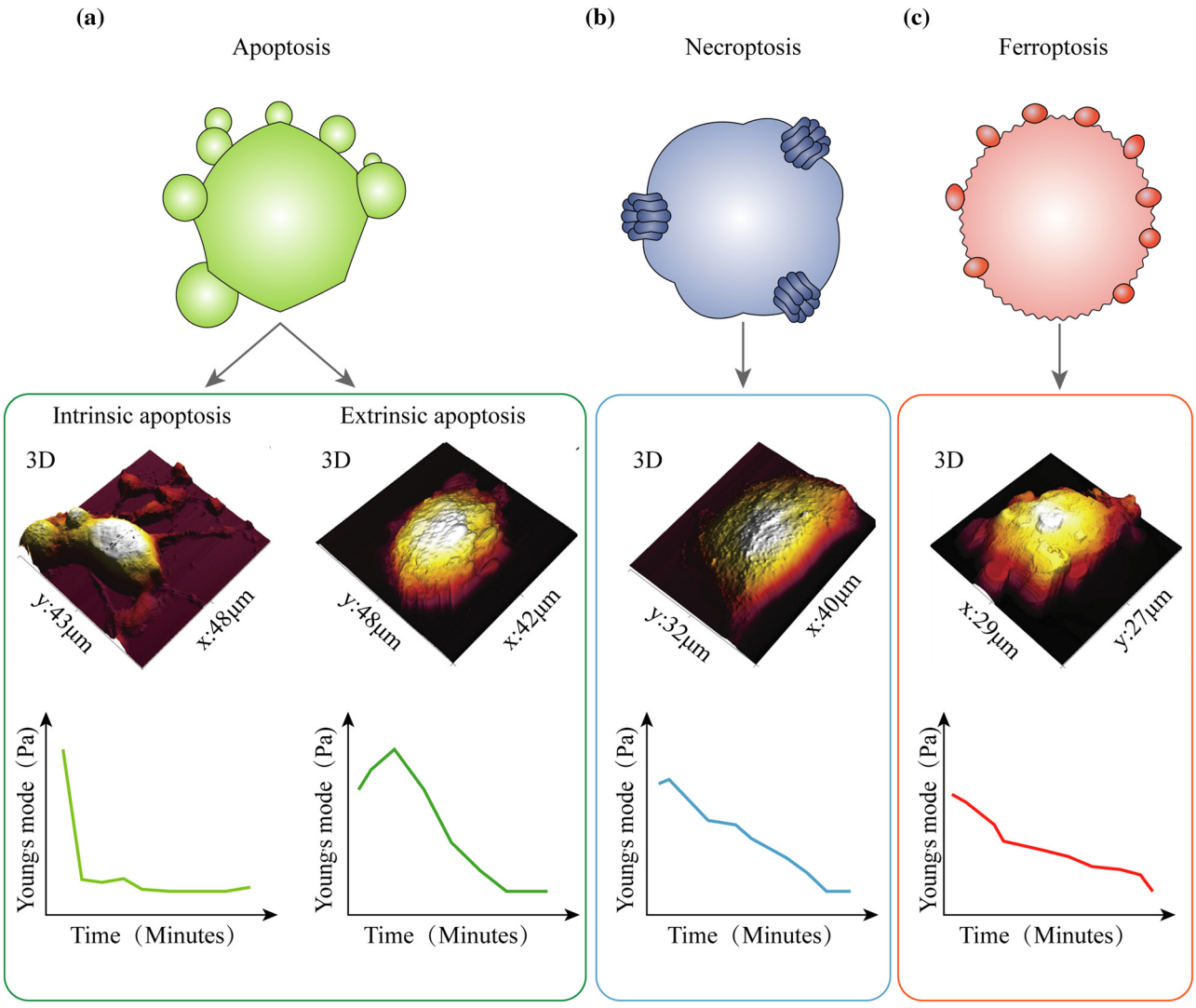

Figure 2: Schematic diagram of different cell death modes morphology (top), AFM imaging 3D topology (middle), and Young's modulus (bottom). (a) Apoptosis, including intrinsic apoptosis and extrinsic apoptosis; (b) necroptosis; and (c) ferroptosis. The AFM imaging 3D topology (middle) and Young's modulus (bottom) are reprinted, with permission, from [30].

of pyroptosis by punching holes in the cell membrane [38]. MLKL is the only known effector molecule associated with necroptosis [98]. Available data suggest that p-MLKL has the potential to create pores in the plasma membrane resulting in membrane rupture [42,43]. Unfortunately, we are not yet able to understand the structure and topology of MLKL in the cell membrane [99]. In addition, the membrane attack complex (MAC), a terminal pathway common to the three complement activation pathways, can also be assembled by soluble monomeric proteins and form killer transmembrane pores that mediate cell death [100]. AFM has successfully imaged the morphology of membrane attack complex structures on the cell membrane (Figure 3a) [92,101]. Similarly, in the past experiments, SEM, TEM, and other microscopes were mostly used to observe the formed membrane pores. However, because of the harsh imaging environment, it is usually difficult to observe clear membrane pore images and the shape of the formed oligomers [102–104]. In contrast, AFM, as a microscope that allows the acquisition of native membrane images at sub-molecular resolution, enables a clearer observation of the dynamic assembly process of transmembrane pores [105]. Therefore, we broadly review relevant studies on the dynamic visualization of membrane pore formation mediated by various molecules by AFM. These studies reveal real-time morphology during pore formation and greatly advance our understanding of pore formation-mediated cell death [106–108].

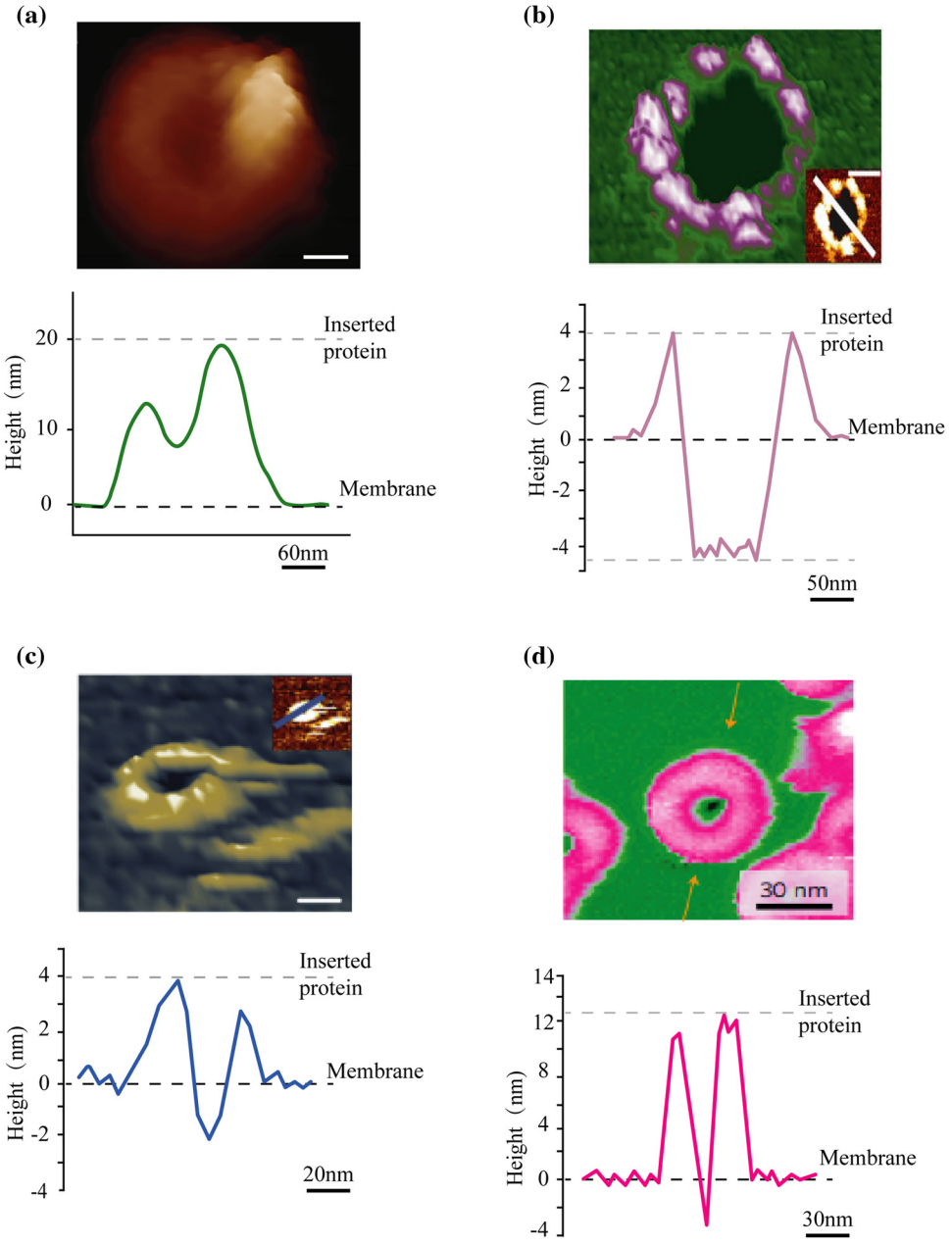

Figure 3: MAC, BAX, BAK, and perforin pore morphological characteristics detected by AFM scanning. AFM imaging 3D topography of the MAC, BAK, BAX, and perforin pore (top of each image). The MAC, BAX, BAK, and perforin molecules around the pore protrude around the membrane plane, as confirmed by the height cross-sections below each image (corresponding to the gray dashed line in the AFM image) (bottom of each image). (a) Open access source, under Creative Commons license, from [92]. (b) Reprinted, with permission, from [93]. (c) Open access source, under Creative Commons license, from [94]. (d) Reprinted, with permission, from [95].

5.1 AFM visualization of BAX/BAK and PFR-mediated apoptosis pore formation

BAX and BAK are pro-apoptotic members of the BCL-2 family required for mitochondrial outer membrane permeability (MOMP) and play a key role in apoptosis [33]. Under normal conditions, BAX and BAK are present in healthy cells in inactive forms. After receiving an apoptotic signal, they are activated and oligomerically inserted into the MOM, which is accompanied by an increase in MOMP, and then BAX and BAK form giant pores [33,34,90]. However, the mechanism of how BAX and BAK aggregate and form apoptotic pores is still not fully understood. A recent study showed that AFM analysis of supported lipid bilayers

(SLBs) prepared from proteoliposomes containing activated BAX monomers revealed that BAX formed linear, arc-shaped, and ring-shaped in SLBs of varying sizes and shapes. In other words, AFM can observe the formation of membrane pores associated with this protein (Figure 3b), which are not uniform in size and shape but are generally circular with diameters between 24 and 176 nm [93]. In the same way, Cosentino *et al.* observed the structure formed by BAK in SLBs and compared it with the pores formed by BAX. BAK also formed straight lines, arcs, and ring structures in SLBs (Figure 3c), but the pores formed by BAK were smaller and more uniform, and the rings had an average pore radius of about 8.12 nm [94].

As a pore-forming protein, PFR can form oligomeric pores in target cell membranes, which allow the entry of pro-apoptotic granzymes, thereby causing apoptosis of target cells [109,110]. Leung *et al.* visualized the PFR nanopore assembly in real time, where PFR first forms loosely but irreversibly bound, short prepore oligomers on target cell membranes. These short oligomers, after insertion into the membrane, recruit additional prepore oligomers, facilitating further assembly to form larger arc- and ring-shaped transmembrane pores (Figure 3d) [95].

5.2 AFM visualization of gasdermin family protein-mediated pyroptosis pore formation

Gasdermin family proteins, as the final executors of pyroptosis, consist of six members in humans, namely GSDMA, GSDMB, GSDMC, GSDMD, GSDME (DFNA5), and PJVK (DFNB59) [111,112]. Among them, GSDMD, as one of the earliest discovered, most widely studied, and most in-depth members of the gasdermin family, can be activated and cleaved by caspase 1/4/5/11 to form N-GSDMD and C-GSDMD. N-GSDMD acts directly on the cell

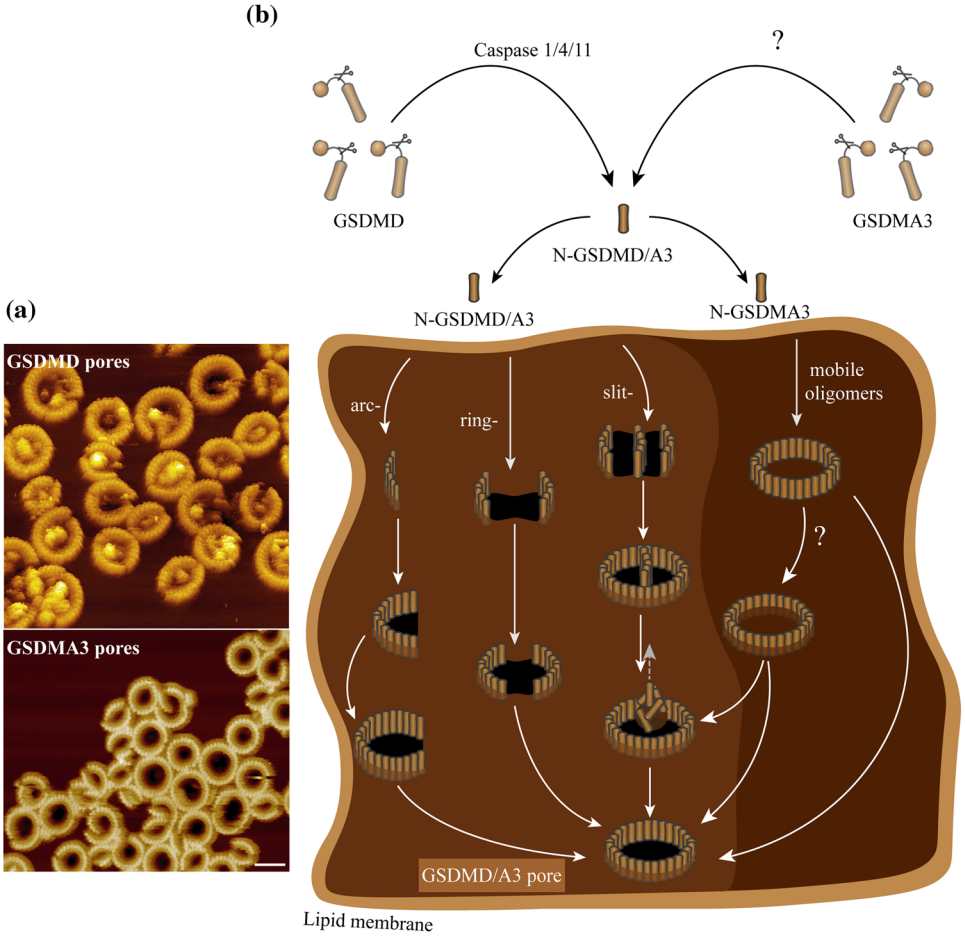

Figure 4: GSDMD/A3 pore formation diagram. (a) AFM images of arc-, slit-, and ring-formed by N-GSDMD/A3 and (b) model of N-GSDMD/A3 oligomerization and pore formation. (a) (Top) Reprinted, with permission, from [91] and (a) (bottom) open access source, under Creative Commons license, from [102].

membrane, forming pores in the membrane and triggering pyroptosis [111–113]. However, how the N-GSDMD domain assembles the pores and the mechanism of penetrating the plasma membrane remains poorly understood. To address this issue, Mulvihil *et al.* applied high-resolution and time-lapse AFM to directly image the pore-forming process of N-GSDMD on supported lipid membranes (SLMs) [91]. Results showed that N-GSDMD released from GSDMD cleavage by caspase-1 can assemble into slit-, ring- and few arc-shaped oligomers (Figure 4a). And each oligomer structure occasionally forms transmembrane pores penetrating the SLMs. The structure height of slit- and ring-shaped oligomers protruding from the SLM is about 3.6 nm, indicating that they are almost completely inserted into the membrane. The analytical data also showed that the diameters of the ring-shaped oligomers were widely distributed between 13.5 and 33.5 nm, with an average value of approximately 22.6 nm [91]. These findings are consistent with the study by Sborgi *et al.* that N-GSDMD binds to lipid membranes and forms arc-, slit-, and ring-shaped oligomers, and the formed arcs and slits may fuse into ring-shaped N-GSDMD oligomers of variable diameter with an average value of 21 nm [103]. On the basis of AFM imaging, it can be speculated that the pathway for N-GSDMD to form pores is roughly as shown in Figure 4b. Furthermore, it is necessary to explore whether the pore-forming activity of GSDMD-N is also present in other gasdermin family members. Mari *et al.* characterized the pore-forming activity of mouse GSDMA3 by high-resolution time-lapse AFM [102]. It was found that GSDMA3 oligomers assemble on the SLMs and remain in a mobile or attached state. And once inserted into the membrane, it oligomerizes to form arc-, slit-, and ring-shaped oligomers, each of which also forms transmembrane pores, the pathway of N-GSDMA3 to form pores is shown in Figure 4b [102]. In addition, Liu *et al.* visualized the pore-forming process of GSDME on the cell membrane by AFM [31]. Overall, these studies collectively suggest that the gasdermin family proteins are the direct and ultimate executor of pyroptosis. The high-resolution information of the pyroptotic pores shows the unique value of AFM in the study of pyroptosis.

5.3 Problems with AFM visualization of membrane pores

To date, AFM has made great progress in visualizing membrane pore formation, but most studies have imaged pores on artificial liposomes or SLMs [91,93,103], and only a few studies have imaged membrane pores on real living cells [31]. This could be due to the strict requirements of high-resolution imaging (nanoscale) and sample preparation problems, imaging in real cell membrane pores is difficult and complicated [31]. Because cell membranes are mainly composed of membrane proteins and phospholipids. Artificial lipid bilayers model (artificial membranes) can simulate cell membranes and keep their function intact [114]. Therefore, the artificial membranes are good alternative to cell membranes. It provides a lot of information about the morphology and properties of a phospholipid bilayer. However, there are still some limitations in the use of artificial liposomes and SLMs for pore visualization, including the lack of a membrane protein-intrinsic cytoskeleton, leading to possible discrepancies among pores in liposomes and SLMs and the actual cell membrane, generating possible errors in observing the dynamics of pore formation [31,115]. For example, related studies have shown that in real cells, PFR-induced pore size is about 200 nm, much larger than that detected from SLMs (about 10–20 nm) [95,115]. In addition, the size of pores formed by GSDMD proteins in real cell membranes and SLMs is also inconsistent [31,91,103]. Therefore, the results obtained using artificial liposomes and SLMs as research subjects may not reflect the relationship between cell membrane pore formation and cell death. To make a better connection between the formation of membrane pores and cell death, the study of real cell membrane pore formation using AFM should be accelerated. However, there is another problem with the visualization of membrane pores by AFM. Although studies are comparing the membrane pores depth with the cytoplasmic membrane thickness to confirm that the membrane pores imaged by AFM are real cell membrane pores and not from membrane depression or folds [31]. We still do not know how to exclude that only hollows were formed as the AFM tip cannot probe the inner part of the cell nor the underneath part of a supported lipid layer.

6 Study of cell death-related molecules using AFM-SMFS

The reasons for different cell death modes are not the same, it has been described above that the changes in morphological and mechanical properties of different cell death modes induced by different substances can be directly detected by AFM. However, as with other imaging techniques, we cannot obtain quantitative information on intermolecular or intramolecular interactions from AFM images,

which also leads us to be unable to fully determine that cell death is induced by a specific substance. And the single-molecule force spectroscopy technique of atomic force microscopy (AFM-SMFS) is a good solution to this problem [116]. Since this technique requires tip-sample interaction, we can achieve this by functionalizing the AFM tip with particular chemical groups/ligands/antibodies. The main methods for attaching specific molecules to the AFM tip include physical adsorption, specific interaction, and chemical coupling (silanization, covalent coupling). In the experimental process, according to the nature of the sample, different connection methods can be used [117–119]. After functionalization, AFM-SMFS allows the measurement of the adhesion and mechanical strength of specific bonds formed between the tip and individual sample molecules. Therefore, AFM can not only be used for imaging but has also become an indispensable measurement tool for studying biological macromolecular interactions.

The rapid development of AFM-SMFS has made it successfully applied to the analysis of single-molecule mechanical properties and intermolecular interactions, including DNA melting and dynamic structural changes [120], the dissociation mechanisms of DNA duplex [121], protein folding and unfolding [122], and interactions between biological macromolecules (protein–protein interaction, protein–nucleic acid interaction, protein–ligand interaction, *etc.*) [123–125]. However, past studies have typically used only one biomolecule to functionalize the AFM tip when applying single-molecule force spectroscopy, but Pfreundschuh *et al.* further developed this technique [126]. Pfreundschuh *et al.* functionalized the AFM tip with two different ligands to map the two binding sites of human G protein-coupled receptors [126]. It can be seen that AFM-SMFS has great prospects in the field of biological research. Therefore, in recent years, AFM-SMFS has also been gradually applied in the field of cell death. pf-80 is an anti-PFR monoclonal antibody that recognizes PFR epitopes without interfering with plasma membrane binding of PFR [109,127]. In studying PFR-induced apoptosis in bulk tumor cells [128] and tumor-repopulating cells (TRC, low flexibility prevents membrane pore formation caused by PFR released by cytotoxic T cells), they attached pf-80 to the AFM tip and examined the adhesion between pf-80 and PFR (Figure 5a, left) [129]. The results showed that in bulk tumor cells, the adhesion between pf-80 and PFR was very high. But in TRC cells, the adhesion between pf-80 and PFR was very low, which may be due to the decreased expression of MYH9 (a motor protein that interacts with PFR) in TRC, which has the function of cross-linking and hardening F-actin. Its reduced expression may lead to a decrease in the interaction force between stable pf-80 and PFR, which ultimately leads to less adhesion between pf-80 and PFR in TRC cells [129]. Epidermal growth factor receptor (EGFR) is a cell transmembrane protein whose overexpression is common in many cancers, which can be activated by binding to epidermal growth factor (EGF). In other words, low expression of EGFR can induce tumor cell death. Resveratrol, as an anti-tumor drug, can inhibit the activity of EGFR, thereby inducing tumor cell death [86,130,131]. Zhang *et al.* used EGF-functionalized AFM probes to study the cell surface EGFR expression changes after treatment with different resveratrol concentrations (Figure 5a, right) [86]. The results showed that there was no significant change in the unbinding force of the low-dose resveratrol-treated group (up to 20 μg ml^{-1}) compared with the untreated group. However, when cells were

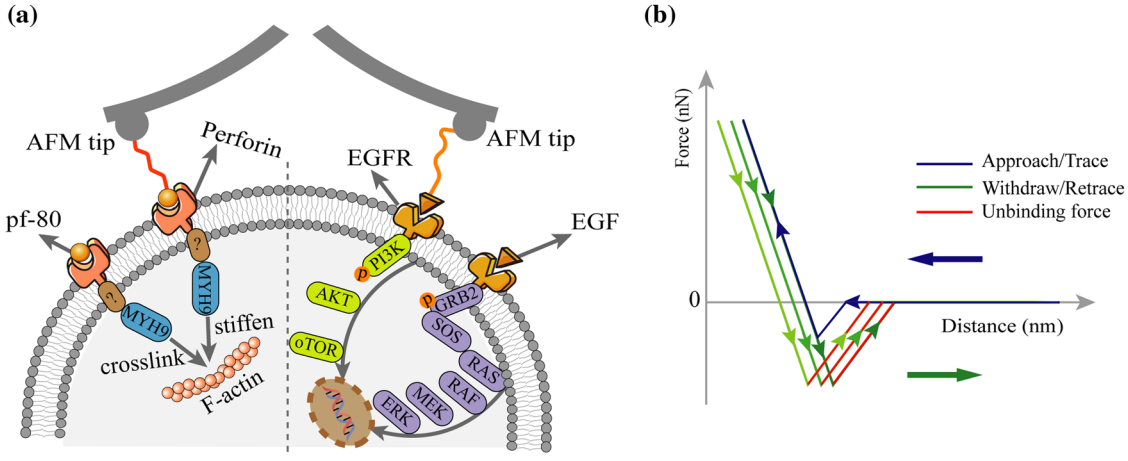

Figure 5: The specific recognition and detection of the molecule related to cell death by single-molecule force spectroscopy technique of atomic force microscopy (AFM-SMFS). (a) Schematic diagram of measuring the interaction between perforin and its monoclonal antibody pf-80, epidermal growth factor (EGF) and its receptor EGFR on the cell membrane by AFM-SMFS technology. (b) Typical force curve of EGF and EGFR interaction with specific unbinding peaks on cancer cells.

treated with 40 μg ml^{-1} resveratrol, the unbinding force was significantly reduced. Furthermore, they also demonstrated that when EGF (100 mg ml^{-1}) is added gently to untreated MCF-7 cells, the interaction forces between EGF and EGFR were specifically blocked (Figure 5b) [86]. Thus, can we apply a similar idea to other cell death processes (Gasdermin family-mediated pyroptosis, MLKL protein-mediated necroptosis) using single-molecule force spectroscopy? This will help us to understand the dynamic changes and mechanisms of single molecules in the process of inducing cell death.

7 Discussion and further perspective

Clearly, AFM has emerged as a powerful imaging tool capable of imaging biological systems at high resolution (nanoscale). AFM topography can be used to characterize the morphological characteristics of different cell death modes. Analysis of cell biomechanical properties can detect the early onset of cell death and the dynamic changes in mechanical properties during death, thereby distinguishing different cell death modes [30]. Notably, AFM is currently the only force measurement technique that can map the nanoscale lateral distribution of individual molecular recognition sites on biological surfaces, which is beyond the reach of traditional biochemical methods [118]. And in recent years, great progress has been made in enhancing the function of AFM, including the development of different AFMs such as multiparametric AFM (MP-AFM) [26], molecular recognition AFM (MR-AFM) [132], multifrequency AFM (MF-AFM) [61], high-speed AFM (HS-AFM) [27], and fluidic force microscopy (FluidFM) [133]. At the same time, to better image and identify the complex structure of some biological systems, AFM can also be combined with other complementary techniques, including OM, fluorescence microscopy, confocal microscopy, super-resolution microscopy, *etc.* The most commonly used combination of AFM is fluorescence microscopy or confocal microscopy [10]. For example, in addressing the limitations of AFM imaging on the cell surface, a study combined AFM with confocal microscopy to directly penetrate the cell membrane and localize to the nucleus through the AFM tip to measure the elasticity of the nucleus [134]. Obviously, this has become a hot spot of current AFM research and a trend of future AFM development. The combination and development of these technologies and functions have greatly enhanced the roles of traditional AFM, but the application of AFM still faces some challenges.

First, how to further improve the spatiotemporal resolution of AFM. At present, conventional AFM is only used to take static snapshots or very slow dynamic processes, because it takes up several minutes to acquire an image of each sample, which is far more than the time required for normal cellular physiological activities. Although high-speed atomic force microscopes with high temporal resolution in the subsecond range have been developed in recent years [135]. However, due to the limitations of its high-speed imaging, this technique is currently only used for imaging small and relatively flat biological samples, such as single proteins and DNA molecules [136,137]. But, for some large biological systems, the spatial resolution of AFM imaging becomes another challenge. For example, the resolution of current AFM imaging of mammalian cells is limited to 50–100 nm, which makes it impossible to observe the individual components of cell-surface machinery [132]. The imaging resolution of microbial cells is slightly higher, but only about 10 nm [10]. So, next, we should consider how AFM can maintain its high temporal resolution and high spatial resolution at the same time when imaging different biological samples.

Second, AFM is low throughput and labor intensive. Current AFM experiments are manual rather than automated. Meanwhile, the traditional AFM takes several minutes or even longer to process one sample, and the next one can only be processed after one sample is processed, which makes the entire operation very time-consuming and labor-intensive. In addition, when measuring the mechanical property changes during cell death based on the force-distance curve, it is usually necessary to measure and analyze thousands of force curves, which will undoubtedly further increase the time and labor consumption. In response to this problem, Chopinet *et al.* provide a novel modality called quantitative imaging™ (QI™), which overcomes the data processing problems associated with acquiring thousands of force curves [138]. However, since this model has not yet been popularized, further researches are needed on related issues. Furthermore, the technical requirements for operators during AFM operation are very strict, especially for dynamic monitoring of living cells, which requires operators to have rich experience and good patience. Therefore, it is imminent to study the AFM of automated operation and simplified operation of data processing systems.

Finally, AFM does not need to be marked to be a double-edged sword. AFM does not need to mark the sample when observing the sample, which is one of the advantages of AFM. However, as the research system becomes more complex, this will turn into a weakness of AFM. For example, many proteins do not exhibit distinct morphologies, which are difficult to distinguish using AFM [8]. Although the existing technology has been able to functionalize the AFM probe, using the tip with specific

molecular modification to specifically recognize the sample molecule. However, this technique is complicated and time-consuming in the molecular modification process, the experimental process is difficult to standardize, and the damage to the tip is unavoidable [139]. Therefore, further development of techniques that allow molecular-specific recognition by AFM is critical for imaging complex biological systems.

Generally speaking, the powerful functions exhibited by AFM make its research prospects in cell death immeasurable. However, as mentioned above, AFM still has many deficiencies in studying the physiological process of cells. Although some novel AFMs have been developed under the joint efforts of experts in multidisciplinary fields, the underlying problems remain unsolved. We expect a new and more powerful AFM that integrates multi-mode, multi-parameter, multi-frequency, and high-speed modes in the future. Coupled with the advancement of various complementary technologies, this will allow us to more clearly explore the unsolved problems of the cell death process and the entire field of biology.

Funding information: This work was supported by the National Natural Science Foundation of China (No. 82273998), the Ministry of Science and Technology of China (National Key R&D Program of China, 2021YFC3002203), and the Funding of Thinkingbiomed Biotechnology (Beijing) Co., Ltd (2022GKF-0667) to Prof. Yanhua Gong.

Author contributions: Ning Li: conception and design of study, investigation, visualization, writing – review and editing, supervision. Li Zhang: investigation, visualization, writing – original draft. Qiao Ou: visualization. Xinyue Wang: visualization. Linyan Xu: visualization. Yanhua Gong: conception and design of study, writing – review and editing, supervision, funding acquisition. All authors have accepted responsibility for the entire content of this manuscript and approved its submission.

Conflict of interest: The authors state no conflict of interest.

References

[1] Bertheloot D, Latz E, Franklin BS. Necroptosis, pyroptosis and apoptosis: An intricate game of cell death. Cell Mol Immunol. 2021;18(5):1106–21.

[2] Ketelut-Carneiro N, Fitzgerald KA. Apoptosis, pyroptosis, and necroptosis-oh my! The many ways a cell can die. J Mol Biol. 2022;434(4):167378.

[3] Tang D, Kang R, Berghe TV, Vandenabeele P, Kroemer G. The molecular machinery of regulated cell death. Cell Res. 2019;29(5):347–64.

[4] Snyder AG, Oberst A. The antisocial network: Cross talk between cell death programs in host defense. Annu Rev Immunol. 2021;39:77–101.

[5] Zemła J, Danilkiewicz J, Orzechowska B, Pabijan J, Seweryn S, Lekka M. Atomic force microscopy as a tool for assessing the cellular elasticity and adhesiveness to identify cancer cells and tissues. Semin Cell Dev Biol. 2018;73:115–24.

[6] Nandi T, Ainavarapu SRK. Applications of atomic force microscopy in modern biology. Emerg Top Life Sci. 2021;5(1):103–11.

[7] Binnig G, Quate CF, Gerber C. Atomic force microscope. Phys Rev Lett. 1986;56(9):930–3.

[8] Li M, Liu L, Xi N, Wang Y, Dong Z, Xiao X, et al. Atomic force microscopy imaging of live mammalian cells. Sci China Life Sci. 2013;56(9):811–7.

[9] Katan AJ, Dekker C. High-speed AFM reveals the dynamics of single biomolecules at the nanometer scale. Cell. 2011;147(5):979–82.

[10] Dufrêne YF, Ando T, Garcia R, Alsteens D, Martinez-Martin D, Engel A, et al. Imaging modes of atomic force microscopy for application in molecular and cell biology. Nat Nanotechnol. 2017;12(4):295–307.

[11] Dufrêne YF. Atomic force microscopy and chemical force microscopy of microbial cells. Nat Protoc. 2008;3(7):1132–8.

[12] Wang J, Wan Z, Liu W, Li L, Ren L, Wang X, et al. Atomic force microscope study of tumor cell membranes following treatment with anti-cancer drugs. Biosens Bioelectron. 2009;25(4):721–7.

[13] Simpson JD, Ray A, Koehler M, Mohammed D, Alsteens D. Atomic force microscopy applied to interrogate nanoscale cellular chemistry and supramolecular bond dynamics for biomedical applications. Chem Commun (Camb). 2022;58(33):5072–87.

[14] Cascione M, De Matteis V, Toma CC, Pellegrino P, Leporatti S, Rinaldi R. Morphomechanical and structural changes induced by ROCK inhibitor in breast cancer cells. Exp Cell Res. 2017;360(2):303–9.

[15] Simon A, Durrieu MC. Strategies and results of atomic force microscopy in the study of cellular adhesion. Micron. 2006;37(1):1–13.

[16] Li M, Liu L, Xi N, Wang Y. Atomic force microscopy studies on cellular elastic and viscoelastic properties. Sci China Life Sci. 2018;61(1):57–67.

[17] Wojcikiewicz EP, Zhang X, Moy VT. Force and compliance measurements on living cells using atomic force microscopy (AFM). Biol Proced Online. 2004;6:1–9.

[18] Merkel R, Nassoy P, Leung A, Ritchie K, Evans E. Energy landscapes of receptor-ligand bonds explored with dynamic force spectroscopy. Nature. 1999;397(6714):50–3.

[19] Lostao A, Lim K, Pallarés MC, Ptak A, Marcuello C. Recent advances in sensing the inter-biomolecular interactions at the nanoscale - A comprehensive review of AFM-based force spectroscopy. Int J Biol Macromol. 2023;238:124089.

[20] Marcuello C, de Miguel R, Lostao A. Molecular recognition of proteins through quantitative force maps at single molecule level. Biomolecules. 2022;12(4):594.

[21] Hansma HG. Surface biology of DNA by atomic force microscopy. Annu Rev Phys Chem. 2001;52:71–92.

[22] Sbrana F, Bongini L, Cappugi G, Fanelli D, Guarino A, Pazzagli L, et al. Atomic force microscopy images suggest aggregation mechanism in cerato-platanin. Eur Biophys J. 2007;36(7):727–32.

[23] Ushiki T, Hitomi J, Ogura S, Umemoto T, Shigeno M. Atomic force microscopy in histology and cytology. Arch Histol Cytol. 1996;59(5):421–31.
[24] Tilwani S, Gandhi K, Narayan S, Ainavarapu SRK, Dalal SN. Disruption of desmosome function leads to increased centrosome clustering in 14-3-3y-knockout cells with supernumerary centrosomes. FEBS Lett. 2021;595(21):2675–90.
[25] Lewis NS, Chouhan G, Belapurkar V, Arora P, Ainavarapu SRK, Sonawane M. A new tension induction paradigm unravels tissue response and the importance of E-cadherin in the developing epidermis. Int J Dev Biol. 2020;64(4-5-6):343–52.
[26] Heu C, Berquand A, Elie-Caille C, Nicod L. Glyphosate-induced stiffening of HaCaT keratinocytes, a peak force tapping study on living cells. J Struct Biol. 2012;178(1):1–7.
[27] Shibata M, Yamashita H, Uchihashi T, Kandori H, Ando T. High-speed atomic force microscopy shows dynamic molecular processes in photoactivated bacteriorhodopsin. Nat Nanotechnol. 2010;5(3):208–12.
[28] Kerr JF, Wyllie AH, Currie AR. Apoptosis: A basic biological phenomenon with wide-ranging implications in tissue kinetics. Br J Cancer. 1972;26(4):239–57.
[29] Afford S, Randhawa S. Apoptosis. Mol Pathol. 2000;53(2):55–63.
[30] Van der Meeren L, Verduijn J, Krysko DV, Skirtach AG. AFM analysis enables differentiation between apoptosis, necroptosis, and ferroptosis in murine cancer cells. iScience. 2020;23(12):101816.
[31] Liu Y, Zhang T, Zhou Y, Li J, Liang X, Zhou N, et al. Visualization of perforin/gasdermin/complement-formed pores in real cell membranes using atomic force microscopy. Cell Mol Immunol. 2019;16(6):611–20.
[32] Efimova I, Catanzaro E, Van der Meeren L, Turubanova VD, Hammad H, Mishchenko TA, et al. Vaccination with early ferroptotic cancer cells induces efficient antitumor immunity. J Immunother Cancer. 2020;8(2):e001369.
[33] Edlich F, Banerjee S, Suzuki M, Cleland MM, Arnoult D, Wang C, et al. Bcl-x(L) retrotranslocates Bax from the mitochondria into the cytosol. Cell. 2011;145(1):104–16.
[34] Cosentino K, García-Sáez AJ. Bax and bak pores: Are we closing the circle? Trends Cell Biol. 2017;27(4):266–75.
[35] Lovell JF, Billen LP, Bindner S, Shamas-Din A, Fradin C, Leber B, et al. Membrane binding by tBid initiates an ordered series of events culminating in membrane permeabilization by Bax. Cell. 2008;135(6):1074–84.
[36] Deng J, Gutiérrez LG, Stoll G, Motiño O, Martins I, Núñez L, et al. Paradoxical implication of BAX/BAK in the persistence of tetraploid cells. Cell Death Dis. 2021;12(11):1039.
[37] Cookson BT, Brennan MA. Pro-inflammatory programmed cell death. Trends Microbiol. 2001;9(3):113–4.
[38] Wang Y, Gao W, Shi X, Ding J, Liu W, He H, et al. Chemotherapy drugs induce pyroptosis through caspase-3 cleavage of a gasdermin. Nature. 2017;547(7661):99–103.
[39] Kayagaki N, Stowe IB, Lee BL, O'Rourke K, Anderson K, Warming S, et al. Caspase-11 cleaves gasdermin D for non-canonical inflammasome signalling. Nature. 2015;526(7575):666–71.
[40] Li N, Wang Y, Wang X, Sun N, Gong YH. Pathway network of pyroptosis and its potential inhibitors in acute kidney injury. Pharmacol Res. 2022;175:106033.
[41] Degterev A, Huang Z, Boyce M, Li Y, Jagtap P, Mizushima N, et al. Chemical inhibitor of nonapoptotic cell death with therapeutic potential for ischemic brain injury. Nat Chem Biol. 2005;1(2):112–9.
[42] Zhang J, Yang Y, He W, Sun L. Necrosome core machinery: MLKL. Cell Mol Life Sci. 2016;73(11–12):2153–63.
[43] Pasparakis M, Vandenabeele P. Necroptosis and its role in inflammation. Nature. 2015;517(7534):311–20.
[44] Dixon SJ, Lemberg KM, Lamprecht MR, Skouta R, Zaitsev EM, Gleason CE, et al. Ferroptosis: an iron-dependent form of non-apoptotic cell death. Cell. 2012;149(5):1060–72.
[45] Linkermann A, Bräsen JH, Darding M, Jin MK, Sanz AB, Heller JO, et al. Two independent pathways of regulated necrosis mediate ischemia-reperfusion injury. Proc Natl Acad Sci U S A. 2013;110(29):12024–9.
[46] Li M, Dang D, Xi N, Wang Y, Liu L. Nanoscale imaging and force probing of biomolecular systems using atomic force microscopy: from single molecules to living cells. Nanoscale. 2017;9(45):17643–66.
[47] Shan Y, Wang H. The structure and function of cell membranes examined by atomic force microscopy and single-molecule force spectroscopy. Chem Soc Rev. 2015;44(11):3617–38.
[48] Arizono M, Idziak A, Quici F, Nägerl UV. Getting sharper: the brain under the spotlight of super-resolution microscopy. Trends Cell Biol. 2023;33(2):148–61.
[49] Liu S, Hoess P, Ries J. Super-resolution microscopy for structural cell biology. Annu Rev Biophy. 2022;51:301–26.
[50] Li W, Kaminski Schierle GS, Lei B, Liu Y, Kaminski CF. Fluorescent nanoparticles for super-resolution imaging. Chem Rev. 2022;122(15):12495–543.
[51] Bond C, Santiago-Ruiz AN, Tang Q, Lakadamyali M. Technological advances in super-resolution microscopy to study cellular processes. Mol Cell. 2022;82(2):315–32.
[52] Rizvi A, Mulvey JT, Carpenter BP, Talosig R, Patterson JP. A close look at molecular self-assembly with the transmission electron microscope. Chem Rev. 2021;121(22):14232–80.
[53] Starodubtseva M, Starodubtsev I, Yegorenkov N, Kuzhel N, Konstantinova E, Chizhik S. Physical-mechanical image of the cell surface on the base of AFM data in contact mode. IOP Conference Series: Materials Science and Engineering. IOP Publishing; 2017. p. 012016.
[54] Chang K-C, Chiang Y-W, Yang C-H, Liou J-W. Atomic force microscopy in biology and biomedicine. Tzu Chi Med J. 2012;24(4):162–9.
[55] Müller DJ, Sass HJ, Müller SA, Büldt G, Engel A. Surface structures of native bacteriorhodopsin depend on the molecular packing arrangement in the membrane. J Mol Biol. 1999;285(5):1903–9.
[56] Engel A, Müller DJ. Observing single biomolecules at work with the atomic force microscope. Nat Struct Biol. 2000;7(9):715–8.
[57] Liang W, Shi H, Yang X, Wang J, Yang W, Zhang H, et al. Recent advances in AFM-based biological characterization and applications at multiple levels. Soft Matter. 2020;16(39):8962–84.
[58] Almonte L, Colchero J. True non-contact atomic force microscopy imaging of heterogeneous biological samples in liquids: topography and material contrast. Nanoscale. 2017;9(8):2903–15.
[59] Li M, Xi N, Liu L. Peak force tapping atomic force microscopy for advancing cell and molecular biology. Nanoscale. 2021;13(18):8358–75.
[60] Ido S, Kimura K, Oyabu N, Kobayashi K, Tsukada M, Matsushige K, et al. Beyond the helix pitch: direct visualization of native DNA in aqueous solution. ACS Nano. 2013;7(2):1817–22.
[61] Ido S, Kimiya H, Kobayashi K, Kominami H, Matsushige K, Yamada H. Immunoactive two-dimensional self-assembly of

monoclonal antibodies in aqueous solution revealed by atomic force microscopy. Nat Mater. 2014;13(3):264–70.
[62] Wegmann S, Jung YJ, Chinnathambi S, Mandelkow EM, Mandelkow E, Muller DJ. Human Tau isoforms assemble into ribbon-like fibrils that display polymorphic structure and stability. J Biol Chem. 2010;285(35):27302–13.
[63] El Kirat K, Burton I, Dupres V, Dufrene YF. Sample preparation procedures for biological atomic force microscopy. J Microscopy. 2005;218(Pt 3):199–207.
[64] Matzke R, Jacobson K, Radmacher M. Direct, high-resolution measurement of furrow stiffening during division of adherent cells. Nat Cell Biol. 2001;3(6):607–10.
[65] Puntheeranurak T, Wildling L, Gruber HJ, Kinne RK, Hinterdorfer P. Ligands on the string: Single-molecule AFM studies on the interaction of antibodies and substrates with the Na+-glucose co-transporter SGLT1 in living cells. J Cell Sci. 2006;119(Pt 14):2960–7.
[66] Harris AR, Charras GT. Experimental validation of atomic force microscopy-based cell elasticity measurements. Nanotechnology. 2011;22(34):345102.
[67] Hockenbery D. Defining apoptosis. Am J Pathol. 1995;146(1):16–9.
[68] Kane AB. Redefining cell death. Am J Pathol. 1995;146(1):1–2.
[69] Elkady AS. Scanning transmitted and reflected light microscopy: A novel microscopy for visualizing biomaterials at interfaces. Micron. 2007;38(8):848–53.
[70] Chen H, Lü JH, Liang WQ, Huang YH, Zhang WJ, Zhang DB. Purification of the recombinant hepatitis B virus core antigen (rHBcAg) produced in the yeast Saccharomyces cerevisiae and comparative observation of its particles by transmission electron microscopy (TEM) and atomic force microscopy (AFM). Micron. 2004;35(5):311–8.
[71] Taatjes DJ, Sobel BE, Budd RC. Morphological and cytochemical determination of cell death by apoptosis. Histochem Cell Biol. 2008;129(1):33–43.
[72] Ryan J, Gerhold AR, Boudreau V, Smith L, Maddox PS. Introduction to modern methods in light microscopy. Methods Mol Biol (Clifton, NJ). 2017;1563:1–15.
[73] Nienhaus K, Nienhaus GU. Where do we stand with super-resolution optical microscopy? J Mol Biol. 2016;428(2 Pt A):308–22.
[74] Kubiak A, Zieliński T, Pabijan J, Lekka M. Nanomechanics in monitoring the effectiveness of drugs targeting the cancer cell cytoskeleton. Int J Mol Sci. 2020;21(22):8786.
[75] Schneider SW, Matzke R, Radmacher M, Oberleithner H. Shape and volume of living aldosterone-sensitive cells imaged with the atomic force microscope. Methods Mol Biol (Clifton, NJ). 2004;242:255–79.
[76] Braet F, Vermijlen D, Bossuyt V, De Zanger R, Wisse E. Early detection of cytotoxic events between hepatic natural killer cells and colon carcinoma cells as probed with the atomic force microscope. Ultramicroscopy. 2001;89(4):265–73.
[77] Hessler JA, Budor A, Putchakayala K, Mecke A, Rieger D, Banaszak Holl MM, et al. Atomic force microscopy study of early morphological changes during apoptosis. Langmuir. 2005;21(20):9280–6.
[78] Wang DC, Chen KY, Tsai CH, Chen GY, Chen CH. AFM membrane roughness as a probe to identify oxidative stress-induced cellular apoptosis. J Biomech. 2011;44(16):2790–4.
[79] Jin H, Zhao H, Liu L, Jiang J, Wang X, Ma S, et al. Apoptosis induction of K562 cells by lymphocytes: an AFM study. Scanning. 2013;35(1):7–11.
[80] Kim KS, Cho CH, Park EK, Jung MH, Yoon KS, Park HK. AFM-detected apoptotic changes in morphology and biophysical property caused by paclitaxel in Ishikawa and HeLa cells. PLoS One. 2012;7(1):e30066.
[81] Su X, Zhou H, Bao G, Wang J, Liu L, Zheng Q, et al. Nanomorphological and mechanical reconstruction of mesenchymal stem cells during early apoptosis detected by atomic force microscopy. Biol Open. 2020;9(3):bio048108.
[82] Hu M, Wang J, Zhao H, Dong S, Cai J. Nanostructure and nanomechanics analysis of lymphocyte using AFM: From resting, activated to apoptosis. J Biomech. 2009;42(10):1513–9.
[83] Jin H, Liang Q, Chen T, Wang X. Resveratrol protects chondrocytes from apoptosis via altering the ultrastructural and biomechanical properties: an AFM study. PLoS One. 2014;9(3):e91611.
[84] Mukherjee C, Bera M, Koti Ainavarapu SR, Sengupta K. Pulling the springs of a cell by single-molecule force spectroscopy. Emerg Top Life Sci. 2021;5(1):77–87.
[85] Pelling AE, Veraitch FS, Pui-Kei Chu C, Nicholls BM, Hemsley AL, Mason C, et al. Mapping correlated membrane pulsations and fluctuations in human cells. J Mol Recognit. 2007;20(6):467–75.
[86] Zhang L, Yang F, Cai JY, Yang PH, Liang ZH. In-situ detection of resveratrol inhibition effect on epidermal growth factor receptor of living MCF-7 cells by Atomic Force Microscopy. Biosens Bioelectron. 2014;56:271–7.
[87] Rotsch C, Radmacher M. Drug-induced changes of cytoskeletal structure and mechanics in fibroblasts: An atomic force microscopy study. Biophys J. 2000;78(1):520–35.
[88] Pelling AE, Veraitch FS, Chu CP, Mason C, Horton MA. Mechanical dynamics of single cells during early apoptosis. Cell Motil Cytoskelet. 2009;66(7):409–22.
[89] Henderson E, Haydon PG, Sakaguchi DS. Actin filament dynamics in living glial cells imaged by atomic force microscopy. Science (New York, NY). 1992;257(5078):1944–6.
[90] McArthur K, Whitehead LW, Heddleston JM, Li L, Padman BS, Oorschot V, et al. BAK/BAX macropores facilitate mitochondrial herniation and mtDNA efflux during apoptosis. Science (New York, NY). 2018;359(6378):eaao6047.
[91] Mulvihill E, Sborgi L, Mari SA, Pfreundschuh M, Hiller S, Müller DJ. Mechanism of membrane pore formation by human gasdermin-D. Embo J. 2018;37(14):e98321.
[92] Parsons ES, Stanley GJ, Pyne ALB, Hodel AW, Nievergelt AP, Menny A, et al. Single-molecule kinetics of pore assembly by the membrane attack complex. Nat Commun. 2019;10(1):2066.
[93] Salvador-Gallego R, Mund M, Cosentino K, Schneider J, Unsay J, Schraermeyer U, et al. Bax assembly into rings and arcs in apoptotic mitochondria is linked to membrane pores. Embo J. 2016;35(4):389–401.
[94] Cosentino K, Hertlein V, Jenner A, Dellmann T, Gojkovic M, Peña-Blanco A, et al. The interplay between BAX and BAK tunes apoptotic pore growth to control mitochondrial-DNA-mediated inflammation. Mol Cell. 2022;82(5):933–49.e9.
[95] Leung C, Hodel AW, Brennan AJ, Lukoyanova N, Tran S, House CM, et al. Real-time visualization of perforin nanopore assembly. Nat Nanotechnol. 2017;12(5):467–73.
[96] Schwarz G, Robert CH. Kinetics of pore-mediated release of marker molecules from liposomes or cells. Biophys Chem. 1992;42(3):291–6.
[97] Baran K, Dunstone M, Chia J, Ciccone A, Browne KA, Clarke CJ, et al. The molecular basis for perforin oligomerization and transmembrane pore assembly. Immunity. 2009;30(5):684–95.

[98] Galluzzi L, Vitale I, Aaronson SA, Abrams JM, Adam D, Agostinis P, et al. Molecular mechanisms of cell death: Recommendations of the Nomenclature Committee on Cell Death 2018. Cell Death Differ. 2018;25(3):486–541.
[99] Flores-Romero H, Ros U, Garcia-Saez AJ. Pore formation in regulated cell death. Embo J. 2020;39(23):e105753.
[100] Bayly-Jones C, Bubeck D, Dunstone MA. The mystery behind membrane insertion: a review of the complement membrane attack complex. Philos Trans R Soc Lond Ser B, Biol Sci. 2017;372(1726):20160221.
[101] Morgan BP, Harris CL. Complement, a target for therapy in inflammatory and degenerative diseases. Nat Rev Drug Discov. 2015;14(12):857–77.
[102] Mari SA, Pluhackova K, Pipercevic J, Leipner M, Hiller S, Engel A, et al. Gasdermin-A3 pore formation propagates along variable pathways. Nat Commun. 2022;13(1):2609.
[103] Sborgi L, Rühl S, Mulvihill E, Pipercevic J, Heilig R, Stahlberg H, et al. GSDMD membrane pore formation constitutes the mechanism of pyroptotic cell death. Embo J. 2016;35(16):1766–78.
[104] Leung C, Dudkina NV, Lukoyanova N, Hodel AW, Farabella I, Pandurangan AP, et al. Stepwise visualization of membrane pore formation by suilysin, a bacterial cholesterol-dependent cytolysin. Elife. 2014;3:e04247.
[105] Frederix PL, Bosshart PD, Engel A. Atomic force microscopy of biological membranes. Biophys J. 2009;96(2):329–38.
[106] Hodel AW, Hammond K, Hoogenboom BW. AFM imaging of pore forming proteins. Methods Enzymol. 2021;649:149–88.
[107] Jiao F, Ruan Y, Scheuring S. High-speed atomic force microscopy to study pore-forming proteins. Methods Enzymol. 2021;649:189–217.
[108] Unsay JD, García-Sáez AJ. AFM to Study Pore-Forming Proteins. Methods Mol Biol (Clifton, NJ). 2019;1886:191–202.
[109] Metkar SS, Marchioretto M, Antonini V, Lunelli L, Wang B, Gilbert RJ, et al. Perforin oligomers form arcs in cellular membranes: a locus for intracellular delivery of granzymes. Cell Death Differ. 2015;22(1):74–85.
[110] Law RH, Lukoyanova N, Voskoboinik I, Caradoc-Davies TT, Baran K, Dunstone MA, et al. The structural basis for membrane binding and pore formation by lymphocyte perforin. Nature. 2010;468(7322):447–51.
[111] Xia S, Hollingsworth LRT, Wu H. Mechanism and regulation of gasdermin-mediated cell death. Cold Spring Harb Perspect Biol. 2020;12(3):a036400.
[112] Broz P, Pelegrín P, Shao F. The gasdermins, a protein family executing cell death and inflammation. Nat Rev Immunol. 2020;20(3):143–57.
[113] Ding J, Shao F. Growing a gasdermin pore in membranes of pyroptotic cells. Embo J. 2018;37(15):e100067.
[114] Wang X, Lu D, Liu Y, Wang W, Ren R, Li M, et al. Electrochemical signal amplification strategies and their use in olfactory and taste evaluation. Biosensors. 2022;12(8):566.
[115] Li J, Liu Y, Yuan Y, Huang B. Applications of atomic force microscopy in immunology. Front Med. 2021;15(1):43–52.
[116] Rief M, Oesterhelt F, Heymann B, Gaub HE. Single molecule force spectroscopy on polysaccharides by atomic force microscopy. Science (New York, NY). 1997;275(5304):1295–7.
[117] Alsteens D, Müller DJ, Dufrêne YF. Multiparametric atomic force microscopy imaging of biomolecular and cellular systems. Acc Chem Res. 2017;50(4):924–31.
[118] Hinterdorfer P, Dufrêne YF. Detection and localization of single molecular recognition events using atomic force microscopy. Nat Methods. 2006;3(5):347–55.
[119] Zhang W, Lü X, Zhang W, Shen J. EMSA and single-molecule force spectroscopy study of interactions between Bacillus subtilis single-stranded DNA-binding protein and single-stranded DNA. Langmuir. 2011;27(24):15008–15.
[120] Zhang W, Dillingham MS, Thomas CD, Allen S, Roberts CJ, Soultanas P. Directional loading and stimulation of PcrA helicase by the replication initiator protein RepD. J Mol Biol. 2007;371(2):336–48.
[121] Burmistrova A, Fresch B, Sluysmans D, De Pauw E, Remacle F, Duwez AS. Force measurements reveal how small binders perturb the dissociation mechanisms of DNA duplex sequences. Nanoscale. 2016;8(22):11718–26.
[122] Brown AE, Litvinov RI, Discher DE, Weisel JW. Forced unfolding of coiled-coils in fibrinogen by single-molecule AFM. Biophys J. 2007;92(5):L39–41.
[123] Dammer U, Hegner M, Anselmetti D, Wagner P, Dreier M, Huber W, et al. Specific antigen/antibody interactions measured by force microscopy. Biophys J. 1996;70(5):2437–41.
[124] Yu J, Jiang Y, Ma X, Lin Y, Fang X. Energy landscape of aptamer/protein complexes studied by single-molecule force spectroscopy. Chem Asian J. 2007;2(2):284–9.
[125] Pérez-Domínguez S, Caballero-Mancebo S, Marcuello C, Martínez-Júlvez M, Medina M. Lostao Nanomechanical A. Study of Enzyme: Coenzyme Complexes: Bipartite Sites in Plastidic Ferredoxin-NADP(+) Reductase for the Interaction with NADP(). Antioxidants (Basel, Switz). 2022;11(3):537.
[126] Pfreundschuh M, Alsteens D, Wieneke R, Zhang C, Coughlin SR, Tampé R, et al. Identifying and quantifying two ligand-binding sites while imaging native human membrane receptors by AFM. Nat Commun. 2015;6:8857.
[127] Praper T, Besenicar MP, Istinic H, Podlesek Z, Metkar SS, Froelich CJ, et al. Human perforin permeabilizing activity, but not binding to lipid membranes, is affected by pH. Mol Immunol. 2010;47(15):2492–504.
[128] Lv J, Liu Y, Cheng F, Li J, Zhou Y, Zhang T, et al. Cell softness regulates tumorigenicity and stemness of cancer cells. Embo J. 2021;40(2):e106123.
[129] Liu Y, Zhang T, Zhang H, Li J, Zhou N, Fiskesund R, et al. Cell softness prevents cytolytic T-cell killing of tumor-repopulating cells. Cancer Res. 2021;81(2):476–88.
[130] Zhang KL, Han L, Chen LY, Shi ZD, Yang M, Ren Y, et al. Blockage of a miR-21/EGFR regulatory feedback loop augments anti-EGFR therapy in glioblastomas. Cancer Lett. 2014;342(1):139–49.
[131] Stewart JR, O'Brian CA. Resveratrol antagonizes EGFR-dependent Erk1/2 activation in human androgen-independent prostate cancer cells with associated isozyme-selective PKC alpha inhibition. Invest N Drugs. 2004;22(2):107–17.
[132] Müller DJ, Dufrêne YF. Atomic force microscopy: a nanoscopic window on the cell surface. Trends Cell Biol. 2011;21(8):461–9.
[133] Guillaume-Gentil O, Potthoff E, Ossola D, Franz CM, Zambelli T, Vorholt JA. Force-controlled manipulation of single cells: from AFM to FluidFM. Trends Biotechnol. 2014;32(7):381–8.
[134] Liu H, Wen J, Xiao Y, Liu J, Hopyan S, Radisic M, et al. In situ mechanical characterization of the cell nucleus by atomic force microscopy. ACS Nano. 2014;8(4):3821–8.
[135] Ando T, Uchihashi T, Scheuring S. Filming biomolecular processes by high-speed atomic force microscopy. Chem Rev. 2014;114(6):3120–88.

[136] Casuso I, Khao J, Chami M, Paul-Gilloteaux P, Husain M, Duneau JP, et al. Characterization of the motion of membrane proteins using high-speed atomic force microscopy. Nat Nanotechnol. 2012;7(8):525–9.

[137] Miyagi A, Ando T, Lyubchenko YL. Dynamics of nucleosomes assessed with time-lapse high-speed atomic force microscopy. Biochemistry. 2011;50(37):7901–8.

[138] Chopinet L, Formosa C, Rols MP, Duval RE, Dague E. Imaging living cells surface and quantifying its properties at high resolution using AFM in QI™ mode. Micron. 2013;48:26–33.

[139] Chtcheglova LA, Hinterdorfer P. Simultaneous AFM topography and recognition imaging at the plasma membrane of mammalian cells. Semin Cell Dev Biol. 2018;73:45–56.